



HAL
open science

Friction induced vibration for an aircraft brake system—Part 2: Non-linear dynamics

Jean-Jacques Sinou, Fabrice Thouverez, Louis Jezequel, Olivier Dereure,
Guy-Bernard Mazet

► To cite this version:

Jean-Jacques Sinou, Fabrice Thouverez, Louis Jezequel, Olivier Dereure, Guy-Bernard Mazet. Friction induced vibration for an aircraft brake system—Part 2: Non-linear dynamics. *International Journal of Mechanical Sciences*, 2006, 48 (5), pp.555-567. 10.1016/j.ijmecsci.2005.12.003 . hal-00207542

HAL Id: hal-00207542

<https://hal.science/hal-00207542>

Submitted on 18 Jan 2008

HAL is a multi-disciplinary open access archive for the deposit and dissemination of scientific research documents, whether they are published or not. The documents may come from teaching and research institutions in France or abroad, or from public or private research centers.

L'archive ouverte pluridisciplinaire **HAL**, est destinée au dépôt et à la diffusion de documents scientifiques de niveau recherche, publiés ou non, émanant des établissements d'enseignement et de recherche français ou étrangers, des laboratoires publics ou privés.

FRICION INDUCED VIBRATION FOR AN AIRCRAFT BRAKE SYSTEM. PART 2 :NON-LINEAR DYNAMICS

J.-J. SINOU ^{1*}, F. THOUVEREZ ¹, L. JEZEQUEL ¹, O. DEREURE ² and G.-B. MAZET ²,

¹Laboratoire de Tribologie et Dynamique des Systèmes UMR CNRS 5513
Ecole Centrale de Lyon, 69134 Ecully, France.

²Messier-Bugatti, Aircraft Braking Division, Zone Aéronautique Louis Bréguet
BP 40, 78140 Vélizy-Villacoublay, France.

ABSTRACT

Non-linear dynamics due to friction induced vibrations in a complex aircraft brake model are investigated. This paper outlines a non-linear strategy, based on the center manifold concept and the rational in order to evaluate the non-linear dynamical behaviour of a system in the neighbourhood of a critical steady-state equilibrium point. In order to obtain time-history responses, the complete set of nonlinear dynamic equations may be integrated numerically. But this procedure is both time consuming and costly to perform when parametric design studies are needed. So it is necessary to use nonlinear analysis : the center manifold approach and the rational approximants are used to obtain the limit cycle of the non-linear system and to study the behaviour of the system in the unstable region. Results from these nonlinear methods are compared with results obtained by integrating the full original system. These non-linear methods appear very interesting in regard to computational time and also necessitate very few computer resources.

NOMENCLATURE

\mathbf{x}	vector of displacement
$\dot{\mathbf{x}}$	vector of velocity
$\ddot{\mathbf{x}}$	vector of acceleration
\mathbf{x}_0	equilibrium point
$\bar{\mathbf{x}}$	small perturbation
\mathbf{C}	damping matrix
\mathbf{K}	stiffness matrix
\mathbf{M}	mass matrix
\mathbf{F}_{NL}	vector of linear and non-linear terms
\mathbf{a}_{ij}	vector of the coefficients of the center manifold
\mathbf{v}_c	vector of center variables
\mathbf{v}_s	vector of stable variables
μ_0	friction coefficient at the Hopf bifurcation point
n_{ij}	coefficients of the denominator of the approximants
d_{ij}	coefficients of the numerator of the approximants

1 INTRODUCTION

Friction induced vibrations are a major concern in a wide variety of mechanical systems. Solving potential vibration problems requires the consideration of the stability analysis and the determination of the non-linear behaviour if the system is unstable. So, thus approaches can be divided onto two parts. As explained in Part I of the paper, the first step is the static problem : the steady-state operating point for the full set of non-linear

equations is obtained by solving them for the equilibrium point. One obtains the linearized whirl equations of motion by introducing small perturbations about the equilibrium point into the non-linear equations. Stability is investigated by determining eigenvalues of this linearized equations for each steady-state operating point of the non-linear system.

The second step is the estimation of the limit cycle. The non-linear dynamic equations can be integrated numerically to obtain a time-history response and this way the limit cycle. However this procedure is too much time consuming. This is why the understanding of the behaviour of the non-linear models with many degrees of freedom requires a simplification and a reduction of the equations due to the fact that the non-linear analysis can be rather expensive and consumes considerable resources both in terms of the computation time and in terms of the data storage requirements. The principal idea for the studies of these dynamical systems, is to use simplification methods to reduce the order of the system and eliminate as many nonlinearities as possible in the system of equations [1-6].

In this paper, the center manifold approach and the rational fractional approximants are used to reduce and simplify the non-linear dynamical system. The principle of the center manifold method is based on the reduction of the dimension of the original system [1-2]: the essential non-linear dynamic system characteristics in the neighbourhood of an equilibrium point is governed by the center manifold associated with the part of the original system characterised by the eigenvalues with zero real parts at the Hopf bifurcation. One chooses the use of the rational approximants [7-10] after applying the center manifold approach. The prime advantage of the rational polynomial approximants is that it may have a greater range of validity than the polynomial approach in any case [7-10]. Moreover, the use of rational approximants allows the computation of an accurate approximation of a function even at values for which the Taylor series of this function diverge [10].

In this paper, results are presented from analyses conducted using the non-linear dynamical model described in Part I of the paper. Firstly, the general expressions of the non-linear model, the methodology for stability analysis, and the determination of the equilibrium point are briefly reviewed. Secondly, the center manifold approach and the rational approximants are used to obtain the limit cycle of the non-linear system and to study the behaviour of the system in the unstable region. Results from these nonlinear methods are compared with results obtained by integrating the full original system.

2 OVERVIEW

As explained in Part I of the paper [11], the non-linear 15-degree-of-freedom whirl system has the form [1]

$$\mathbf{M}\ddot{\mathbf{x}} + \mathbf{C}\dot{\mathbf{x}} + \mathbf{K}\mathbf{x} = \mathbf{F}_{\text{pressure}} + \mathbf{F}_{\text{NL}}(\mathbf{x}) \quad (1)$$

where $\ddot{\mathbf{x}}$, $\dot{\mathbf{x}}$ and \mathbf{x} are the acceleration, velocity, and displacement response 15-dimensional vectors of the degrees-of-freedom, respectively. \mathbf{M} is the mass matrix, \mathbf{C} is the damping matrix and \mathbf{K} is the stiffness matrix. $\mathbf{F}_{\text{pressure}}$ is the vector force due to brake command and \mathbf{F}_{NL} contains moreover the quadratic and cubic non-linear terms.

In Part I of the paper, the first step is the static problem: the steady state operating point for the full set of non-linear equations is obtained by their solving at the equilibrium point. Stability is investigated by calculating the Jacobian of the system at the equilibrium point [12]. This equilibrium point \mathbf{x}_0 is obtained by solving the non-linear static equations for a given net brake hydraulic pressure. This equilibrium point satisfies the following conditions:

$$\mathbf{K}\mathbf{x}_0 = \mathbf{F}_{\text{pressure}} + \mathbf{F}_{\text{NL}}(\mathbf{x}_0) \quad (2)$$

Next, the second step is the estimation of the limit cycle amplitudes near the Hopf bifurcation point, if the system is unstable. The Hopf bifurcation point is defined as follows [13]

$$\begin{aligned} \text{Re}(\lambda_{\text{center}}(\mu))\Big|_{\mathbf{x}=\mathbf{x}_0, \mu=\mu_0} &= 0 \\ \text{Re}(\lambda_{\text{non-center}}(\mu))\Big|_{\mathbf{x}=\mathbf{x}_0, \mu=\mu_0} &\neq 0 \\ \frac{d}{d\mu}(\text{Re}(\lambda(\mu)))\Big|_{\mathbf{x}=\mathbf{x}_0, \mu=\mu_0} &\neq 0 \end{aligned} \quad (3)$$

where the eigenvalues λ_{center} have a pair of purely imaginary part while all of the other eigenvalues $\lambda_{\text{non-center}}$ have nonzero real parts at $(\mathbf{x} = \mathbf{x}_0, \mu = \mu_0)$.

The non-linear dynamic equations can be integrated numerically to obtain a time-history response and this way the limit cycle amplitude. However this procedure is too much time consuming. So the center manifold reduction and the rational approximants will be applied in order to obtain equations for the limit cycle.

3 NONLINEAR ANALYSIS

3.1 Classical approach

The time-history responses of the nonlinear dynamic system (1) can be calculated by using classical fourth-order Runge-Kutta algorithm, as illustrated in Figures 1-4. One observes that the displacement and velocity growth until one obtains the periodic oscillations. Figure 5 shows the evolution of the associated limit cycle amplitudes. This procedure is rather expensive and consumes considerable resources both in terms of the computation time and in terms of the data storage requirements. So, the understanding of the behaviour of this non-linear system requires a simplification and a reduction of the equations. In order to obtain the non-linear simplified system, the center manifold approach and the rational approximants will be used.

The complete non-linear expressions are expressed at the Hopf bifurcation point and by considering the equilibrium point \mathbf{x}_0 for small perturbations $\bar{\mathbf{x}}$ (with $\mathbf{x} = \mathbf{x}_0 + \bar{\mathbf{x}}$). The determination of the Hopf bifurcation point is determined by considering the equation (2).

The complete non-linear equations can be written as follow:

$$\mathbf{M}\ddot{\bar{\mathbf{x}}} + \mathbf{C}\dot{\bar{\mathbf{x}}} + \mathbf{K}\bar{\mathbf{x}} = \mathbf{F}_{\text{NL}}(\bar{\mathbf{x}}) \quad (4)$$

where $\ddot{\bar{\mathbf{x}}}$, $\dot{\bar{\mathbf{x}}}$ and $\bar{\mathbf{x}}$ are the acceleration, velocity, and displacement response of the degrees-of-freedom, respectively. \mathbf{M} is the mass matrix, \mathbf{C} is the damping matrix and \mathbf{K} is the stiffness matrix. $\mathbf{F}_{\text{NL}}(\bar{\mathbf{x}})$ contains the non-linear terms near the Hopf bifurcation point for a given equilibrium point.

3.2 The center manifold theory

The principle of the center manifold method is based on the reduction of the dimension of the original system (Holmes [7], Nayfeh [8-9]): the essential non-linear dynamic system characteristics in the neighbourhood of an equilibrium point is governed by the center manifold associated with the part of the original system characterised by the eigenvalues with zero real parts at the Hopf bifurcation.

One considers reduction to lower dimensional problem by the consideration of the center manifold theory. The non-linear equations are written in state variables and one projects these equations on the basis of its eigenvectors

$$\begin{cases} \dot{\mathbf{v}}_c = \mathbf{J}_c(\hat{\mu})\mathbf{v}_c + \mathbf{G}(\mathbf{v}_c, \mathbf{v}_s, \hat{\mu}) \\ \dot{\mathbf{v}}_s = \mathbf{J}_s(\hat{\mu})\mathbf{v}_s + \mathbf{H}(\mathbf{v}_c, \mathbf{v}_s, \hat{\mu}) \\ \dot{\hat{\mu}} = 0 \end{cases} \quad (5)$$

where $\mathbf{v}_c \in \mathbb{R}^2$ and $\mathbf{v}_s \in \mathbb{R}^{n-2}$ (with $n=30$ in this case). By considering the physically interesting case of the stable equilibrium losing stability, it may assume that \mathbf{v}_s contains the variables associated to the eigenvalues λ with negative real part. \mathbf{G} and \mathbf{H} are polynomial non-linear functions.

Then, the expression of the variables \mathbf{v}_s can be expressed as a function of \mathbf{v}_c [14]. One defines $\mathbf{v}_s = \mathbf{h}(\mathbf{v}_c, \hat{\mu})$ as a power series in $(\mathbf{v}_c, \hat{\mu})$ of degree m , without constant and linear terms ($m \geq 2$):

$$\mathbf{v}_s = \mathbf{h}(\mathbf{v}_c, \hat{\mu}) = \sum_{p=i+j+l=2}^m \sum_{j=0}^p \sum_{l=0}^p \mathbf{a}_{ijl} v_{c1}^i v_{c2}^j \hat{\mu}^l \quad (6)$$

where \mathbf{a}_{ijl} are vectors of constant coefficients. This $(n-2)$ -dimensional function \mathbf{h} is substituted into the second equation of (6) and then these results are combined with the first equation of (6).

By considering the tangency conditions at the fixed point $(\mathbf{0}, \mathbf{0}, 0)$ to the center eigenspace, one obtains

$$\begin{cases} D_{\mathbf{v}_c, \hat{\mu}}(\mathbf{h}(\mathbf{v}_c, \hat{\mu}))(\mathbf{J}_c \mathbf{v}_c + \mathbf{G}(\mathbf{v}_c, \mathbf{h}(\mathbf{v}_c, \hat{\mu}), \hat{\mu})) - \mathbf{J}_s \mathbf{h}(\mathbf{v}_c, \hat{\mu}) - \mathbf{H}(\mathbf{v}_c, \mathbf{h}(\mathbf{v}_c, \hat{\mu}), \hat{\mu}) = 0 \\ \mathbf{h} = \mathbf{0} \\ D_{\mathbf{v}_c} h_i(\mathbf{0}) = 0 \quad \text{for } 1 \leq i \leq n-2 \\ \frac{\partial \mathbf{h}}{\partial \hat{\mu}} = 0 \end{cases} \quad (7)$$

where h_i ($1 \leq i \leq n-2$) are the scalar components of \mathbf{h} .

After \mathbf{h} is identified [11], it is resubstituted into the first equation of (7) to obtain the reduced order structural dynamic model, which is only a function of \mathbf{v}_c :

$$\begin{cases} \dot{\mathbf{v}}_c = \mathbf{J}_c(\hat{\mu}) \mathbf{v}_c + \mathbf{G}(\mathbf{v}_c, \mathbf{v}_s, \hat{\mu}) \\ \dot{\hat{\mu}} = 0 \\ \mathbf{v}_s = \mathbf{h}(\mathbf{v}_c, \hat{\mu}) = \sum_{p=i+j+l=2}^m \sum_{j=0}^p \sum_{l=0}^p \mathbf{a}_{ijl} v_{c1}^i v_{c2}^j \hat{\mu}^l \end{cases} \quad (8)$$

Here, one reduces the number of equations of the non-linear system from 30 to 2.

3.3 Fractional approximants

The center manifold equations can have complicated non-linear terms, which can be simplified using further non-linear methods. The main objective in the rational approximants is to approximate the non-linear terms by using rational polynomial approximants [7-10]. The use of the rational approximants allows to simplify the non-linear system and to obtain limit cycles more easily and rapidly. Moreover, the interest of these rational approximants is that they need less terms than the associated Taylor series in order to obtain an accurate approximation of the limit cycle amplitudes. In any case, the rational approximation has a greater range of validity than the polynomial one.

Let $f(x, y)$ be a function of 2-variables defined by a formal power series expansion

$$f(x, y) = \sum_{i=0}^{\infty} \sum_{j=0}^{\infty} c_{ij} x^i y^j = \sum_{(i,j) \in S} c_{ij} x^i y^j \quad (9)$$

where $S = \{(i, j) | i \in \mathbb{N}^+, j \in \mathbb{N}^+\}$.

In this paper, one considers symmetric-off-diagonal (SOD) rational approximants [3-4] to $f(x, y)$ of the form

$$[m/n]_f(x, y) = \frac{\sum_{(i,j) \in S_m} n_{ij} x^i y^j}{\sum_{(i,j) \in S_n} d_{ij} x^i y^j} \quad (10)$$

where $S_m = \{(i, j) | 0 \leq i \leq m, 0 \leq j \leq m\}$ and $S_n = \{(i, j) | 0 \leq i \leq n, 0 \leq j \leq n\}$. There are $(m+1)^2 + (n+1)^2$ unknown coefficients in (10). d_{00} can be normalised to unity and the other coefficients n_{ij} and d_{ij} are then related by matching terms in (9) and (10). It is useful to introduce a lattice space diagram to indicate the regions in which the terms $x^i y^j$ are to be matched, as illustrated in Figure 6. One defines the following sets (with $m' = \min(m, n)$ and $n' = \max(m, n)$):

$$P = \{(p, p) | 0 \leq p \leq m'\} \quad (11)$$

$$R_{1;p} = \{(p, p)\} \cup \{(\alpha, p) | p \leq \alpha \leq m'\} \cup \{(p, \beta) | p \leq \beta \leq m'\} \quad (12)$$

$$R_{2;p} = \{(\alpha, p) | m' < \alpha \leq n'\} \cup \{(p, \beta) | m' < \beta \leq n'\} \quad (13)$$

$$R_{3;p} = \{(\alpha, p) | n' < \alpha \leq m+n-p\} \cup \{(p, \beta) | n' < \beta \leq m+n-p\} \quad (14)$$

$$R_{4;p} = \{(m+n-p+1, p), (p, m+n-p+1)\} \quad (15)$$

$$S_1 = S_m \cap S_n, \quad S_2 = S_m \cup S_n \setminus S_1 \quad (16, 17)$$

$$S_3 = \bigcup_{p \in P} R_{3;p}, \quad S_4 = \bigcup_{p \in P} R_{4;p}, \quad S_5 = S_2 \setminus \bigcup_{p \in P} R_{2;p} \quad (18, 19, 20)$$

By multiplying the difference between $f(x, y)$ and $[m/n]_f(x, y)$ by the denominator of $[m/n]_f(x, y)$, one obtains

$$\left(\sum_{(i,j) \in S_n} d_{ij} x^i y^j \right) \times \left(\sum_{(i,j) \in S} c_{ij} x^i y^j \right) - \sum_{(i,j) \in S_m} n_{ij} x^i y^j = \sum_{(i,j) \in S} e_{ij} x^i y^j \quad (21)$$

with

$$e_{ij} = 0 \quad (i, j) \in R_{1;p} \cup R_{2;p} \cup R_{3;p} \text{ and } \sum_{p \neq 0} e_{m+n-p+1, p} + e_{p, m+n-p+1} = 0 \quad (22 \text{ and } 23)$$

Next, the equations obtained by matching coefficients in (24) are

$$\sum_{\psi \in S_n} d_{\psi} c_{\rho-\psi} = n_{\rho} \quad \rho \in S_m \quad (24)$$

$$\sum_{\psi \in S_n} d_{\psi} c_{\rho-\psi} = n_{\rho} \quad \rho \in (S_n \setminus S_m) \cup S_3 \quad (25)$$

$$\sum_{\psi \in R_{3;p}} \sum_{\rho \in S_n} d_{\psi} c_{\rho-\psi} = 0 \quad \rho \in P \quad (26)$$

The developed form of the previous linear equations (24-26) may be rewritten in the following way for the first and second center manifold variables previously defined

$$d_{k,00} = 1 \quad (27)$$

$$\sum_{i=0}^{\alpha} \sum_{j=0}^{\beta} d_{k,ij} c_{k,\alpha-i,\beta-j} = n_{\alpha\beta} \quad 0 \leq \alpha \leq m, 0 \leq \beta \leq m \quad (28)$$

$$\sum_{i=0}^{\alpha} \sum_{j=0}^n d_{k,ij} c_{k,\alpha-i,\beta-j} = 0 \quad 0 \leq \alpha < m, m \leq \beta \leq m+n-\alpha \quad (29)$$

$$\sum_{i=0}^n \sum_{j=0}^{\beta} d_{k,ij} c_{k,\alpha-i,\beta-j} = 0 \quad m \leq \alpha \leq m+n-\beta, 0 \leq \beta < m \quad (30)$$

$$\sum_{i=0}^{\sigma} \sum_{j=0}^n (d_{k,ij} c_{k,\sigma-i,m+n+1-\sigma-j} + d_{k,ij} c_{k,m+n+1-\sigma-i,\sigma-j}) = 0 \quad 1 \leq \sigma \leq n \quad (31)$$

with $1 \leq k \leq 2$. After normalizing $d_{k,00}$ to unity as indicated in the first equation of (27), there are $k \times ((m+1)^2 + (n+1)^2 - 1)$ unknown coefficients in equations (28-31). The first step is the determination of the $k \times ((n+1)^2 - 1)$ unknown coefficients $d_{k,ij}$. It is useful to introduce the lattice space diagram to indicate the regions in which the terms x and y are to be matched, as illustrated in Figure 6. $k \times (n(n+1)/2)$ equations arise from each of (29) and (30) which are obtained by matching terms of the two triangular regions S_3 . Now, $k \times n$ equations arise from (31) obtained by equating to zero the sums of the coefficients of the pairs $x^{\alpha} y^{\beta}$ and $x^{\beta} y^{\alpha}$. These pairs are indicated in the regions S_4 by the two associated points A_i (with $i = 1, 2, \dots, N$). Finally, the $k \times ((n+1)^2 - 1)$ coefficients $d_{k,ij}$ can be achieved by solving $k \times ((n+1)^2 - 1)$ linear equations (29-31). Next, the $k \times (m+1)^2$ coefficients $n_{k,ij}$ may be found by directly solving the equations (28); the associated terms $x^{\alpha} y^{\beta}$ are in the regions $S_1 \cup S_2 \cup S_5$. In conclusion, It is easy to obtain the unknown coefficients $n_{k,ij}$ and $d_{k,ij}$ from equations (28-31). However, the resolution of the $k \times ((m+1)^2 + (n+1)^2)$ linear equations may be both time

consuming and costly to perform, and require a very large storage space. So it is possible to apply a special process, called the "prong method" [9], to rapidly compute the coefficients by taking the equations (27-31) in a special order. This computational process reduces the calculation of all the coefficients to linear algebra with a lower triangular block by block resolution which greatly simplifies the determination of the coefficients $n_{k,ij}$ and $d_{k,ij}$.

The first step in the "prong method" consists of determining the denominator coefficients $d_{k,ij}$. As explained previously, the determination of this coefficients can be achieved by considering the pairs of two regions S_3 and S_4 that may be shown in Figure 5. However, it may be observed that the $k \times (n+1)$ coefficients $d_{k,i,0}$ (with $0 \leq i \leq n$) are matched by considering the segment of the lattice space ($m+1 \leq \alpha \leq m+n, \beta=0$). Similarly, the $k \times (n+1)$ coefficients $d_{0,j}$ (with $0 \leq j \leq N$) are located on the segment. Then, by normalizing equation $d_{k,0,0} = 1$, the two previous systems may be written in the following way

$$\begin{bmatrix} c_{k,0,m-n+1} & \cdots & c_{k,0,m} & 0 & \cdots & 0 & c_{k,0,m+1} \\ \vdots & & \vdots & \vdots & & \vdots & \vdots \\ c_{k,0,m} & \cdots & c_{k,0,m+n-1} & 0 & \cdots & 0 & c_{k,0,m+n} \\ 0 & \cdots & 0 & c_{k,m-n+1,0} & \cdots & c_{k,m,0} & c_{k,m+1,0} \\ \vdots & & \vdots & \vdots & & \vdots & \vdots \\ 0 & \cdots & 0 & c_{k,m,0} & \cdots & c_{k,m+n-1,0} & c_{k,m+n,0} \\ 0 & \cdots & 0 & 0 & \cdots & 0 & 1 \end{bmatrix} \begin{Bmatrix} d_{k,0,n} \\ \vdots \\ d_{k,0,1} \\ d_{k,n,0} \\ \vdots \\ d_{k,1,1} \\ d_{k,0,0} \end{Bmatrix} = \begin{Bmatrix} 0 \\ \vdots \\ 0 \\ 0 \\ \vdots \\ 0 \\ 1 \end{Bmatrix} \quad (32)$$

This system may be written in the compact form

$$\mathbf{A}_{k,0} \mathbf{d}_{k,0} = \mathbf{u}_k \quad (33)$$

where $\mathbf{d}_{k,0}$ defines the $(2 \times n + 1)$ -dimensional vector of the coefficients $d_{k,0,0}$, $d_{k,0,i}$ and $d_{k,i,0}$ (with $1 \leq i \leq n$). \mathbf{u}_k defines the column vector of dimension $(2 \times n + 1)$ with unity in the $(2 \times n + 1)^{th}$ place and zeros elsewhere. Finally, the k^{th} vector $\mathbf{d}_{k,0}$ may be obtained by considering

$$\mathbf{d}_{k,0} = \mathbf{A}_{k,0}^{-1} \mathbf{u}_k \quad (34)$$

Next, the $k \times (2 \times n - 1)$ coefficients $d_{k,1,1}$, $d_{k,i,1}$ and $d_{k,i,i}$ (with $2 \leq i \leq n$) are obtained by matching terms on the segments of the lattice space ($m+1 \leq \alpha \leq m+n, \beta=1$) and ($\alpha=1, m+1 \leq \beta \leq m+n$) (defined in the two regions S_3 by the lines marked (1) in Figure 7), and on the symmetrized linked pair of points $(1, m+n)$ and $(m+n, 1)$ (defined by the two points A_1 in Figure 7). These equations of the determination of these coefficients may be written in matrix form

$$\mathbf{B}_{k,11} \mathbf{d}_{k,0} + \mathbf{A}_{k,1} \mathbf{d}_{k,1} = \mathbf{0} \quad (35)$$

where $\mathbf{B}_{k,11} \mathbf{d}_{k,0}$ defines the $(2 \times n - 1)$ -dimensional vector of known quantity. $\mathbf{d}_{k,1}$ and $\mathbf{A}_{k,1}$ are given by

$$\mathbf{d}_{k,1} = \{d_{k,1,n} \quad \cdots \quad d_{k,1,2} \quad d_{k,n,1} \quad \cdots \quad d_{k,2,1} \quad d_{k,1,1}\}^T \quad (36)$$

$$\mathbf{A}_{k,1} = \begin{bmatrix} c_{k,0,m-n+1} & \cdots & c_{k,0,m-1} & 0 & \cdots & 0 & c_{k,0,m} \\ \vdots & & \vdots & \vdots & & \vdots & \vdots \\ c_{k,0,m-1} & \cdots & c_{k,0,m+n-3} & 0 & \cdots & 0 & c_{k,0,m+n-2} \\ 0 & \cdots & 0 & c_{k,m-n+1,0} & \cdots & c_{k,m-1,0} & c_{k,m,0} \\ \vdots & & \vdots & \vdots & & \vdots & \vdots \\ 0 & \cdots & 0 & c_{k,m-1,0} & \cdots & c_{k,m+n-3,0} & c_{k,m+n-2,0} \\ c_{k,0,m} & \cdots & c_{k,0,m+n-2} & c_{k,m,0} & \cdots & c_{k,m+n-2,0} & c_{k,m+n-1,0} + c_{k,0,m+n-1} \end{bmatrix} \quad (37)$$

. Finally, the k^{th} vector $\mathbf{d}_{k,1}$ may be obtained by considering relation

$$\mathbf{d}_{k,1} = -\mathbf{A}_{k,1}^{-1} \mathbf{B}_{k,11} \mathbf{d}_{k,0} \quad (38)$$

By using an iterative process, the overall system of the equations involving the determination of the $\mathbf{d}_{k,p}$ vector with $p=1,\dots,n$ may be defined by

$$\begin{bmatrix} \mathbf{A}_{k,0} & \mathbf{0} & \cdots & \cdots & \cdots & \mathbf{0} \\ \mathbf{B}_{k,11} & \mathbf{A}_{k,1} & \ddots & & & \vdots \\ \mathbf{B}_{k,21} & \mathbf{B}_{k,22} & \mathbf{A}_{k,2} & \ddots & & \vdots \\ \mathbf{B}_{k,31} & \mathbf{B}_{k,32} & \mathbf{B}_{k,33} & \mathbf{A}_{k,3} & \ddots & \vdots \\ \vdots & \vdots & \vdots & \ddots & \ddots & \mathbf{0} \\ \mathbf{B}_{k,n1} & \mathbf{B}_{k,n2} & \mathbf{B}_{k,n3} & \cdots & \mathbf{B}_{k,nn} & \mathbf{A}_{k,n} \end{bmatrix} \begin{Bmatrix} \mathbf{d}_{k,0} \\ \mathbf{d}_{k,1} \\ \mathbf{d}_{k,2} \\ \mathbf{d}_{k,3} \\ \vdots \\ \mathbf{d}_{k,n} \end{Bmatrix} = \begin{Bmatrix} \mathbf{u}_n \\ \mathbf{0} \\ \mathbf{0} \\ \mathbf{0} \\ \vdots \\ \mathbf{0} \end{Bmatrix} \quad (39)$$

Then, the $(2n-2i+1)$ -dimensional vector $\mathbf{d}_{k,i}$ (with $i=1,\dots,n$) may be obtained by a block by block inversion process called the ‘‘prong method’’. Finally, the $k \times (m+1)^2$ numerator coefficients $n_{k,ij}$ may be determined by considering the block by block iterative process

$$\begin{Bmatrix} \mathbf{n}_{k,0} \\ \mathbf{n}_{k,1} \\ \mathbf{n}_{k,2} \\ \mathbf{n}_{k,3} \\ \vdots \\ \vdots \\ \mathbf{n}_{k,m} \end{Bmatrix} = \begin{bmatrix} \mathbf{C}_{k,0} & \mathbf{0} & \cdots & \cdots & \cdots & \mathbf{0} \\ \mathbf{D}_{k,11} & \mathbf{C}_{k,1} & \ddots & & & \vdots \\ \mathbf{D}_{k,21} & \mathbf{D}_{k,22} & \mathbf{C}_{k,2} & \ddots & & \vdots \\ \mathbf{D}_{k,31} & \mathbf{D}_{k,32} & \mathbf{D}_{k,33} & \mathbf{C}_{k,3} & \ddots & \vdots \\ \vdots & \vdots & \vdots & \ddots & \ddots & \mathbf{0} \\ \mathbf{D}_{k,m1} & \mathbf{D}_{k,m2} & \mathbf{D}_{k,m3} & \cdots & \mathbf{D}_{k,mm} & \mathbf{C}_{k,m} \end{bmatrix} \begin{Bmatrix} \mathbf{d}_{k,0} \\ \mathbf{d}_{k,1} \\ \mathbf{d}_{k,2} \\ \mathbf{d}_{k,3} \\ \vdots \\ \vdots \\ \mathbf{d}_{k,m} \end{Bmatrix} \quad (40)$$

where the matrices $\mathbf{C}_{k,i}$ (with $i=0,\dots,m$) and $\mathbf{D}_{k,ij}$ (with $i=1,\dots,m$ and $j=1,\dots,m$) and the vector $\mathbf{d}_{k,i}$ (with $i=0,\dots,n$) are known.

3.4 Numerical simulations

In this section, the center manifold and the rational approximants are applied to the aircraft brake system (1). The basic parameters chosen for the parametric studies are: $P/P_{max} = 0.3$; $\alpha/\alpha_{max} = 0.0875$; $\eta/\eta_{max} = 0.04$; $K_{rr}/K_{rrmax} = 0.78$.

First of all, approximations of orders 2 and 3 for the center manifold reduction are considered. Figures 8 illustrate the comparison of the limit cycle amplitudes of the original non-linear 15-degree-of-freedom system calculated by using classical fourth-order Runge-Kutta algorithm, and approximated by applying the center manifold of orders 2 or 3, respectively. It may be observed that an approximation of order 2 is not sufficient to describe with low errors the non-linear behaviour of the system. However, using an approximation of order 3 allows good approximations of the limit cycles, even if the axial limit cycles of the stator and rotor (Figures 8(a) and 8(e)) are not exactly the same than those obtained for the original system. It may be observed that the more higher the polynomial order of the stable variables are, the more interesting the estimate limit cycles of the reduced system is, but the more costly and time consuming the computations are. Consequently, the center manifold reduction is validated and allows the reduction of equations of the original system from 30 to 2 (in state variables) without losing the dynamics of the non-linear behaviour of the original system.

This is well known that the sole use of the center manifold approach is not very convenient due to the number of non-linear terms generated during the reduction of the system.

In order to simplify the non-linear expressions of the reduced system, the rational fractional approximants are applied. Effectively, they require fewer terms than the associated Taylor series in order to obtain an accurate estimation of the non-linear expressions.

Using the symmetric-off-diagonal (SOD) rational approximants, the previous non-linear system (8), written by considering the center manifold approach, can be written as follow

$$\dot{\mathbf{v}}_c = \mathbf{f}^{\text{NL}}(\mathbf{v}_c) = \left\{ \begin{array}{cc} \frac{\sum_{i=0}^m \sum_{j=0}^m n_{1,ij} v_{c1}^i v_{c2}^j}{\sum_{i=0}^n \sum_{j=0}^n d_{1,ij} v_{c1}^i v_{c2}^j} & \frac{\sum_{i=0}^m \sum_{j=0}^m n_{2,ij} v_{c1}^i v_{c2}^j}{\sum_{i=0}^n \sum_{j=0}^n d_{2,ij} v_{c1}^i v_{c2}^j} \end{array} \right\}^T \quad (41)$$

where \mathbf{f}^{NL} represents the non-linear expression in symmetric-off-diagonal (SOD) rational approximants form. The determinations of the coefficients $n_{1,ij}$, $n_{2,ij}$ (for $0 \leq i \leq m$ and $0 \leq j \leq m$) and $d_{1,ij}$, $d_{2,ij}$ (for $0 \leq i \leq n$ and $0 \leq j \leq n$) are obtained by using the procedure defined previously.

Figures 9-23 illustrate the comparison of the original limit cycle amplitudes and the estimated limit cycle amplitudes by applying Padé approximation ([2/2], [4/2], [5/4], and [6/6]). First if all, it may be observed that the fractional approximants [2/2] give a good estimation of the limit cycles for all degree-of-freedom. This clearly indicates that the fractional approximants require fewer terms than the center manifold expressions for obtaining an accurate approximation of the limit cycles. Moreover, the limit cycles obtained for the higher fractional approximants appears to be not acceptable (for example Padé approximants [5/4] on Figures 9-23) or diverge (as indicated in Table 1). These results illustrates that, in some cases, the rational approximants may give a lower estimation of the limit cycles even if the number of the retained non-linear terms increases.

Then, the limit cycles obtained by using the rational approximants appears to be closed to the original limit cycles even if the polynomial approximation of the center manifold are not sufficient to obtain a very good estimate of non-linear contributions of the original system and the associated limit cycles. This last point may be clearly illustrated by comparing Figures 8(a), 8(e) (i.e. limit cycles by using the center manifold approximations), and Figures 9, 13 (i.e. limit cycles by applying the Padé approximants).

Finally, results for another set of parameters (for $P/P_{\max}=0.1$) are undertaken in order to show one of the most difficult points due to the center manifold reduction. In this case, the second order approximation of the center manifold diverge, since the approximation of the stable variable is not sufficient, as illustrated in Figures 24 and 25. However, applying the third-order polynomial approximation and the $[3/2]_r(\mathbf{v}_c)$ symmetric-off-diagonal rational permit to obtain a very good approximation of the limit cycles amplitudes, as illustrated in Figure Figures 26. In this case, one has only 28 non-linear terms by using the rational approximants. So the center manifold theory and the rational approximants appear very interesting in regard to computational time and also necessitate very few computer resources, as indicated in Table 2.

Moreover, this example illustrates that one of the most difficult points using the center manifold reduction is the determination of polynomial approximations and the estimate of the minimal power that defines the expressions of stable variable versus center variables (as indicated in equation (8)). Effectively, obtaining the coefficients associated with the stable variable may pose serious computational difficulties. So even if the more complex the expressions of the stable variables are, the more interesting the non-linear reduced system is, in practice, the estimate of the lower power of the stable variables that allows us to obtain a good approximation of the non-linear limit-cycles may be one of the most important key points. Then, this is why the extension of the center manifold approach by using the rational approximants is very interesting due to the fact that the rational approximants require fewer terms than the associated Taylor series and augment the domain of validity the series obtained by the center manifold reduction [10].

4 SUMMARY AND CONCLUSION

A nonlinear analysis of mode aircraft brake whirl has been developed. The center manifold theory and the rational approximants are used in order to reduce and to simplify the non-linear system while retaining the essential features of the dynamic behavior near the Hopf bifurcation point. Excellent agreements are found between the results obtained by these methods and the complete solution of the non-linear system. However, these methods are very interesting when time history response solutions of the full set of non-linear equations are time consuming to perform when extensive parametric design studies are needed.

Moreover, the interest of these rational approximants is that they need less terms than the associated Taylor series in order to obtain an accurate approximation of the limit cycle amplitudes; the rational approximation has a greater range of validity than the polynomial one obtained by using the center manifold approach.

ACKNOWLEDGMENTS

The authors would like to thank Messier-Bugatti for permission to publish this work.

REFERENCES

- [1] J-J. Sinou, Synthèse Non-Linéaire des Systèmes Vibrants – Application aux systèmes de freinage, Thèse de doctorat, Ecole Centrale de Lyon, 2002.
- [2] J. Guckenheimer and P. Holmes. *Nonlinear Oscillations, Dynamical Systems, and Bifurcations of vector Fields*, Springer-Verlag, 1986.
- [3] A.H. Nayfeh and D.T. Mook. *Nonlinear Oscillations*. John Wiley & Sons, 1995.
- [4] A.H. Nayfeh and B. Balachandran. *Applied Nonlinear Dynamics: Analytical, Computational and Experimental Methods*, John Wiley & Sons, 1995.
- [5] Jézéquel, L. and Lamarque, C.H., 'Analysis of Non-linear Dynamical Systems by the Normal Form Theory', in *Journal of Sound and Vibration*, 1991, 149, pp. 429-459.
- [6] Yu, P., 'Computation of normal forms via a perturbation technique', *Journal of Sound and Vibration*, 1998, 211, pp. 19-38.
- [7] G.A. Baker and P. Graves-Morris, *Cambridge University Press*, Padé Approximants, 1996.
- [8] C. Brezinski, *Padé Type Approximation and General Orthogonal Polynomials*, INSNM, vol. 50, Birkhauser-Verlag, Basel, 1980.
- [9] R. Hughes Jones *Journal of Approximation Theory* , 16, 201-233. General rational approximants in N-variables, 1976.
- [10] J-J. Sinou, F. Thouverez, and L. Jézéquel 2003 *Journal of Nonlinear Dynamics*, 33: 267-282. Extension of the Center Manifold Approach, Using the Rational Fractional Approximants, Applied to Non-linear Stability Analysis.
- [11] J-J. Sinou, O. Dereure, G-B. Mazet, F. Thouverez and L. Jézéquel , *International Journal of Mechanical Sciences*, Friction Induced Vibration for an Aircraft Brake System. Part 1: Experimental Approach and Stability Analysis. Revised paper.
- [12] J-J. Sinou, F. Thouverez, L. Jézéquel and G-B. Mazet, Friction, Instability and Parametric Studies of a Nonlinear Model for an Aircraft Brake Whirl Analysis, DETC2001/VIB-21726, *ASME, September 9-13, Pittsburgh, Pennsylvania*, 2001.
- [13] J.E. Marsden, J.E., and McCracken, M., *Applied Mathematical Sciences. The Hopf Bifurcation and its Applications*, Spring-Verlag, 1976.
- [14] J. Carr, *Application of Center Manifold*, Springer-Verlag, New-York, 1981.

Padé approximants	Limit cycles estimation
[2/2]	Good approximation
[3/2]	Divergence
[3/3]	Divergence
[4/2]	Good approximation
[4/3]	Divergence
[4/4]	Divergence
[5/2]	Bad approximation
[5/3]	Bad approximation
[5/4]	Good approximation
[5/5]	Good approximation
[6/6]	Good approximation

Table 1: Comparison between the original system and the Padé reduced system

	Original system	Reduced system
CPU Time	5 hours	5 minutes
Number of degree-of-freedom in states variables	30	2
Number of non-linear terms	108000	28

Table 2: Comparison between the original system and the reduced system (for $P/P_{\max}=0.1$)

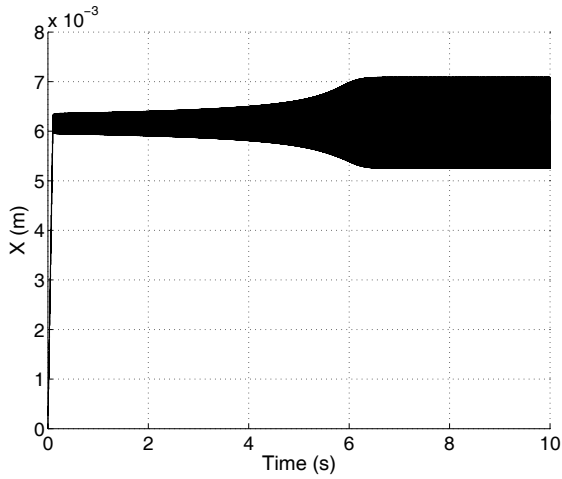


Figure 1: Axial displacement of the rotor ($\mu = 1.01\mu_0$)

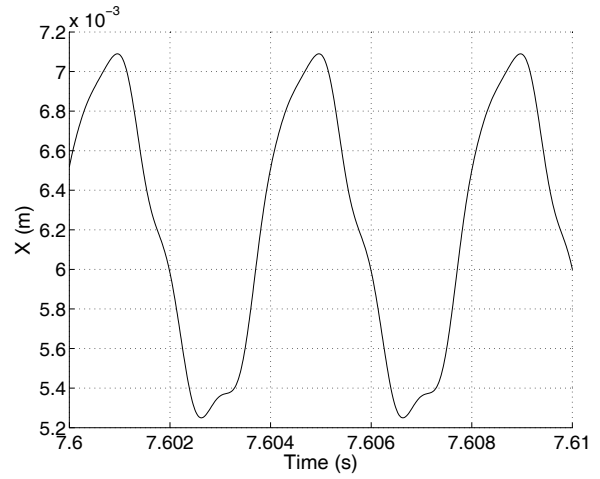


Figure 2: Zoom of the axial displacement of the rotor ($\mu = 1.01\mu_0$)

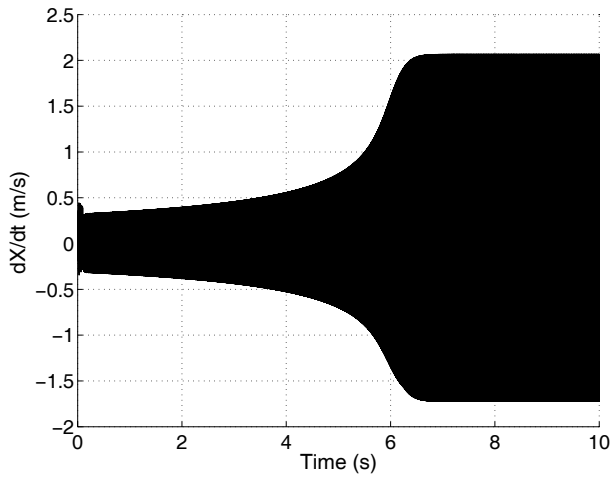


Figure 3 : Axial velocity of the rotor ($\mu = 1.01\mu_0$)

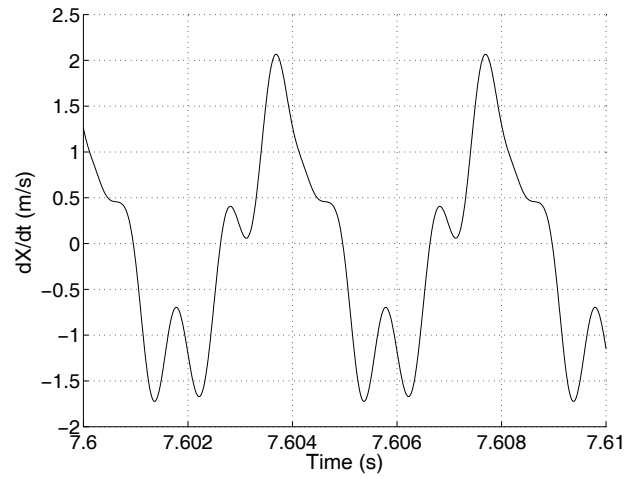


Figure 4 : Zoom of the axial velocity of the rotor ($\mu = 1.01\mu_0$)

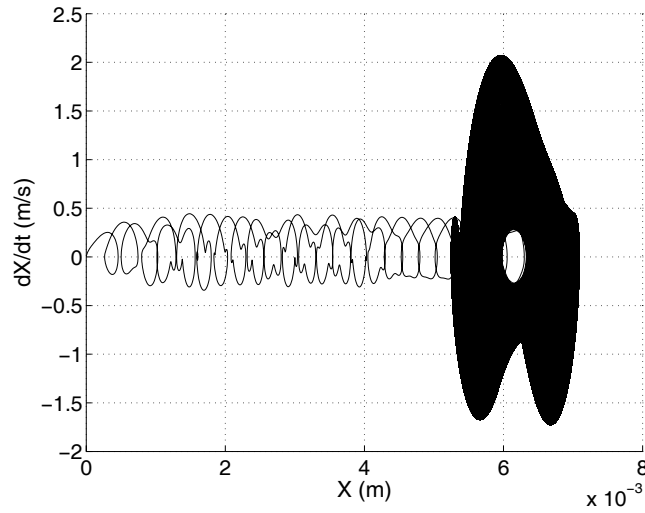


Figure 5: Limit cycle ($\mu = 1.01\mu_0$)

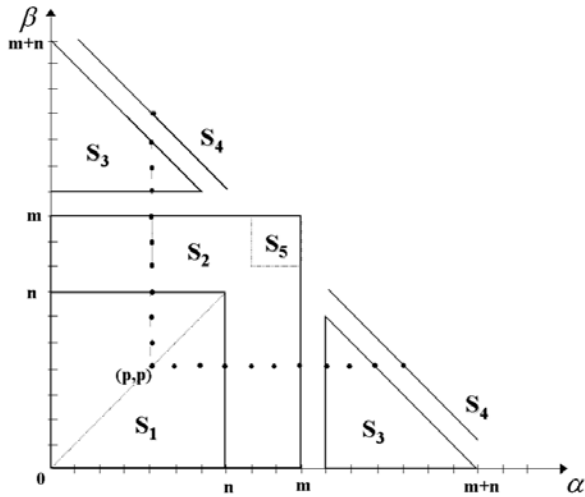


Figure 6 : Lattice space

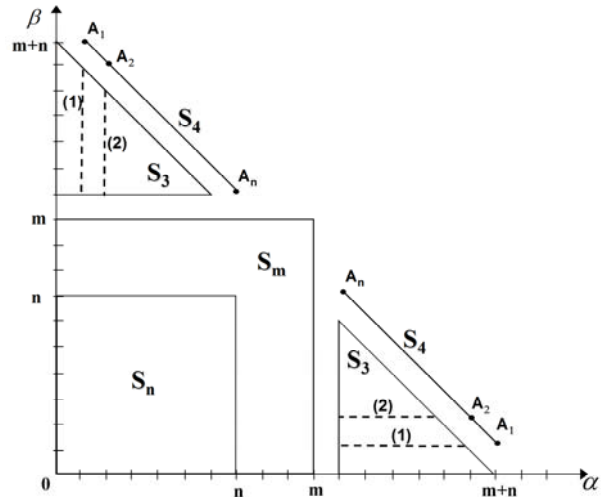
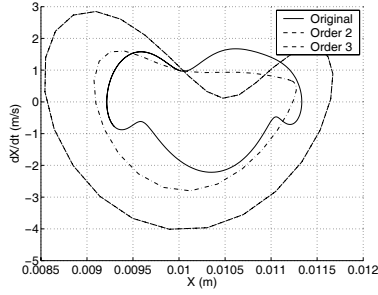
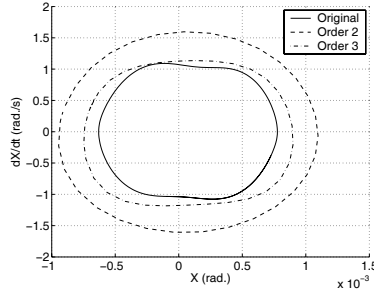


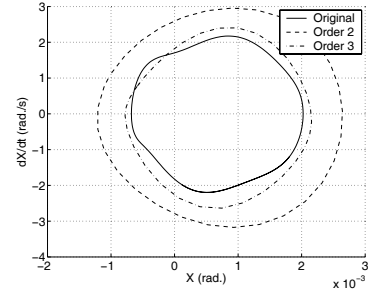
Figure 7: The "prong method" and associated regions in the lattice space



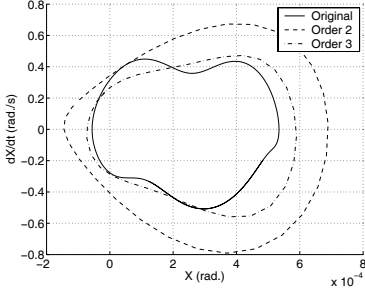
(a) Limit cycle (x_s, \dot{x}_s)



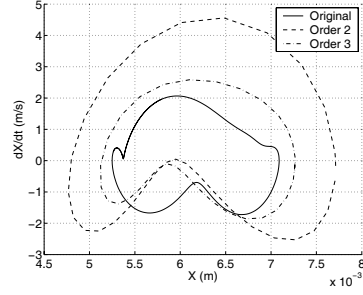
(b) Limit cycle $(\theta_s, \dot{\theta}_s)$



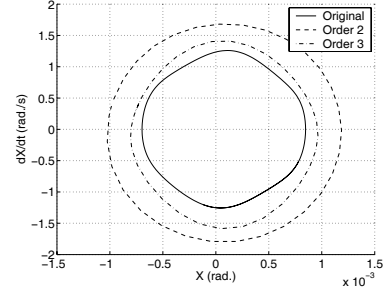
(c) Limit cycle $(\psi_s, \dot{\psi}_s)$



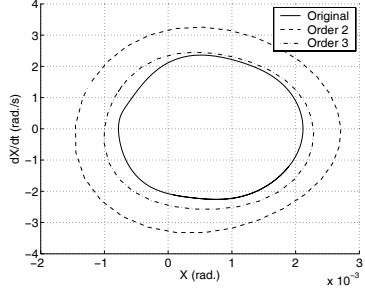
(d) Limit cycle $(\phi_s, \dot{\phi}_s)$



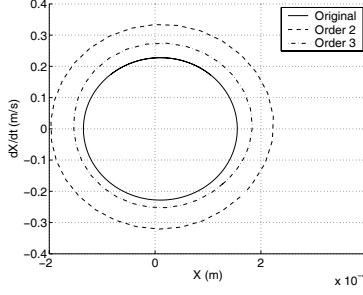
(e) Limit cycle (x_r, \dot{x}_r)



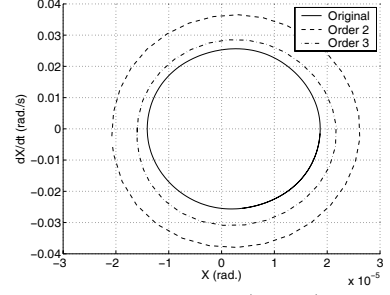
(f) Limit cycle $(\theta_r, \dot{\theta}_r)$



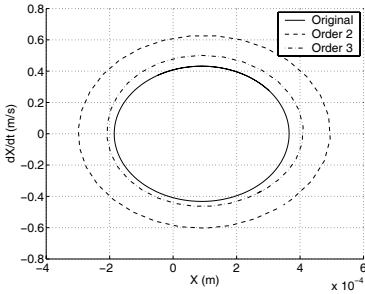
(g) Limit cycle $(\psi_r, \dot{\psi}_r)$



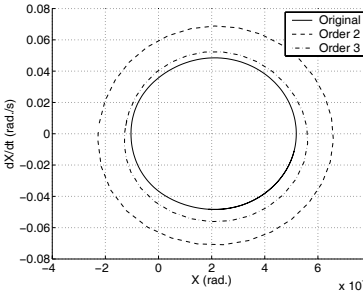
(h) Limit cycle (y_b, \dot{y}_b)



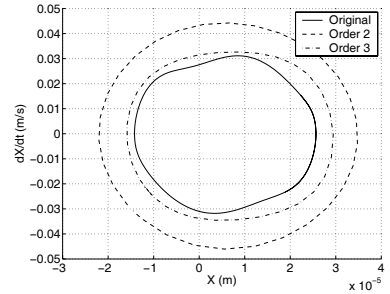
(i) Limit cycle $(\theta_b, \dot{\theta}_b)$



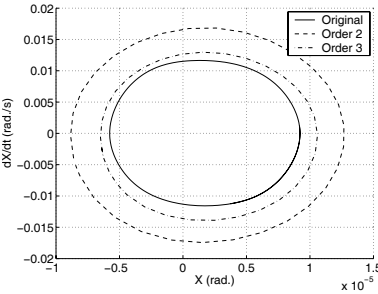
(j) Limit cycle (z_b, \dot{z}_b)



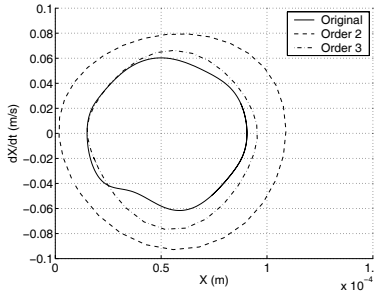
(k) Limit cycle $(\psi_b, \dot{\psi}_b)$



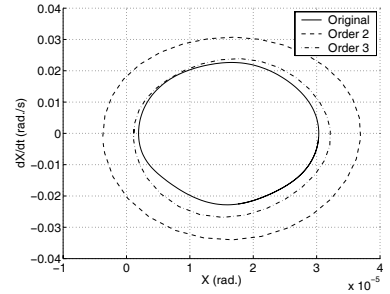
(l) Limit cycle (y_a, \dot{y}_a)



(m) Limit cycle $(\theta_a, \dot{\theta}_a)$



(n) Limit cycle (z_a, \dot{z}_a)



(o) Limit cycle $(\psi_a, \dot{\psi}_a)$

Figure 8: Comparison between the original system and the reduced system obtained by using the center manifold

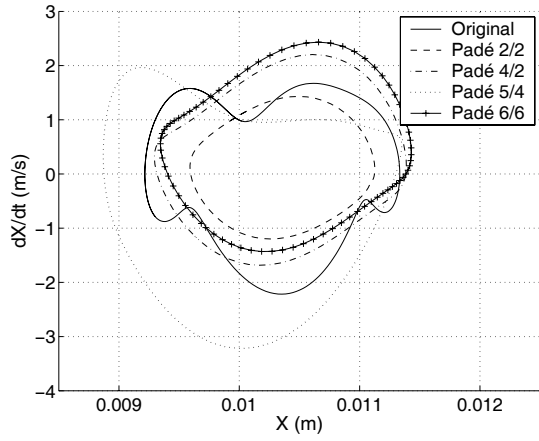


Figure 9: Limit cycle (x_s, \dot{x}_s) for $\mu = 1.01\mu_0$

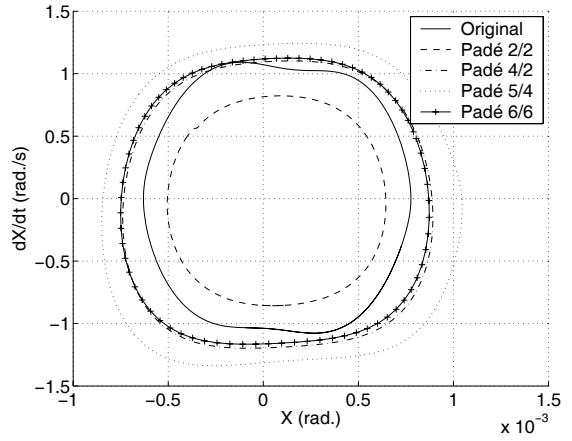


Figure 10: Limit cycle $(\theta_s, \dot{\theta}_s)$ for $\mu = 1.01\mu_0$

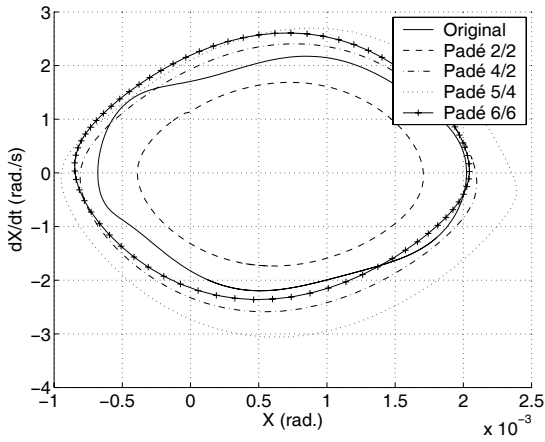


Figure 11: Limit cycle $(\psi_s, \dot{\psi}_s)$ for $\mu = 1.01\mu_0$

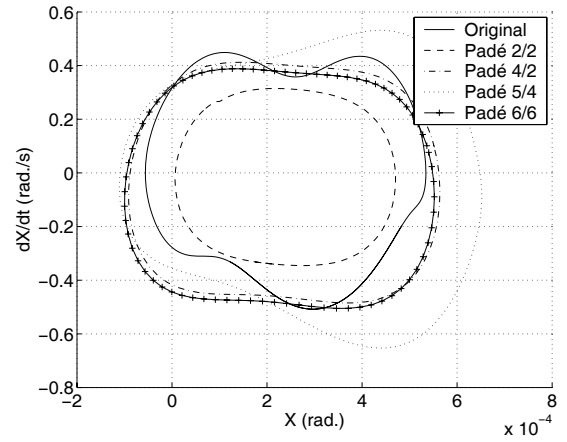


Figure 12: Limit cycle $(\phi_s, \dot{\phi}_s)$ for $\mu = 1.01\mu_0$

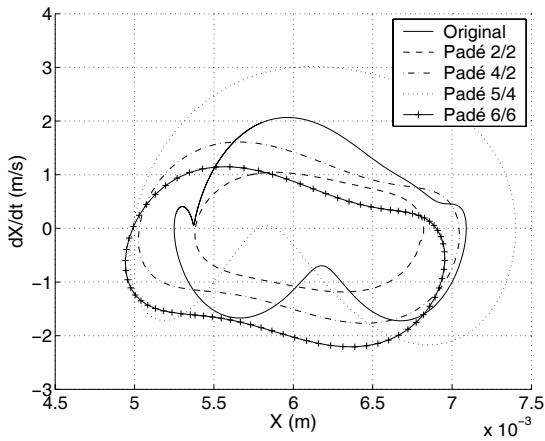


Figure 13: Limit cycle (x_r, \dot{x}_r) for $\mu = 1.01\mu_0$

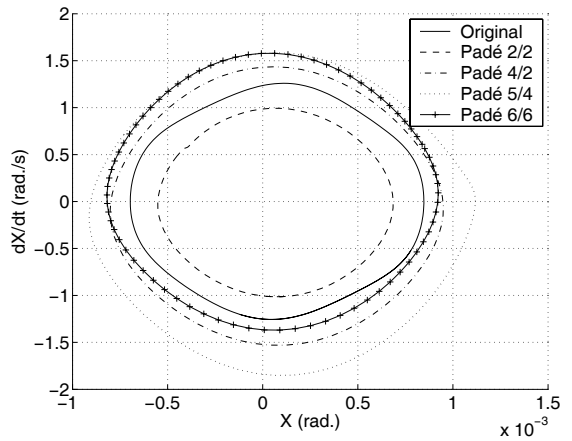


Figure 14: Limit cycle $(\theta_r, \dot{\theta}_r)$ for $\mu = 1.01\mu_0$

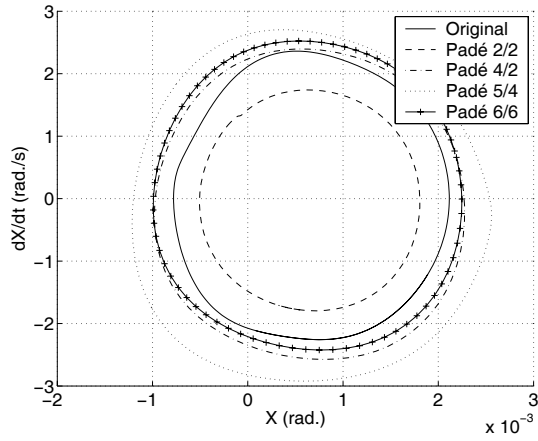


Figure 15: Limit cycle $(\psi_r, \dot{\psi}_r)$ for $\mu = 1.01\mu_0$

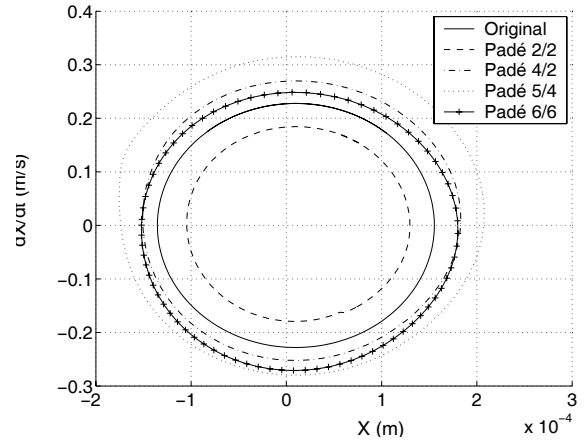


Figure 16: Limit cycle (y_b, \dot{y}_b) for $\mu = 1.01\mu_0$

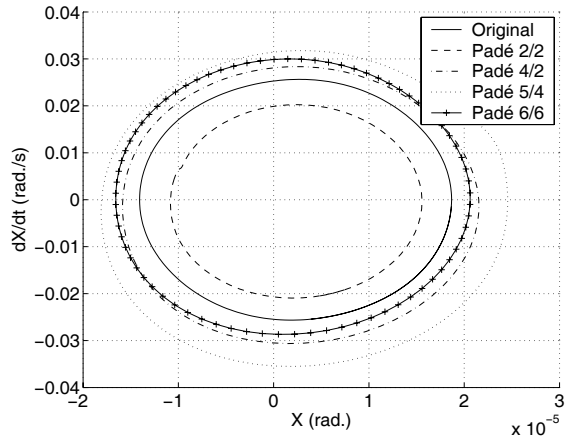


Figure 17: Limit cycle $(\theta_b, \dot{\theta}_b)$ for $\mu = 1.01\mu_0$

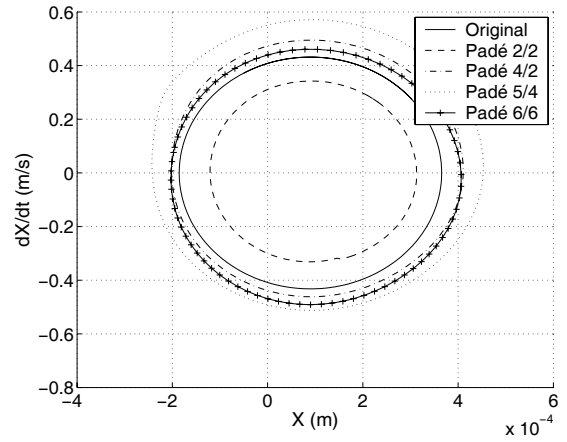


Figure 18: Limit cycle (z_b, \dot{z}_b) for $\mu = 1.01\mu_0$

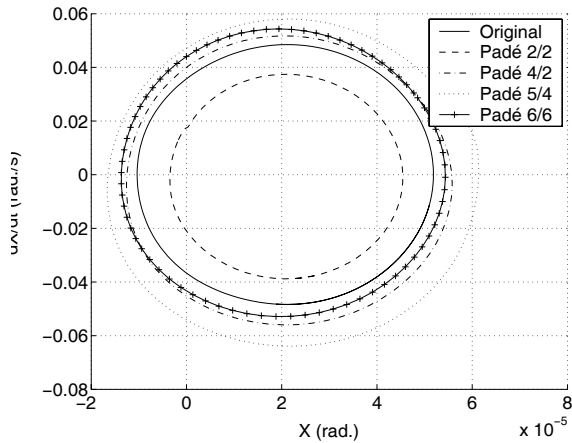


Figure 19: Limit cycle $(\psi_b, \dot{\psi}_b)$ for $\mu = 1.01\mu_0$

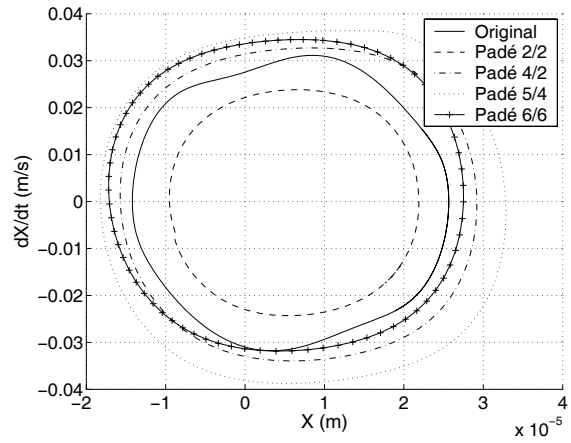


Figure 20: Limit cycle (y_a, \dot{y}_a) for $\mu = 1.01\mu_0$

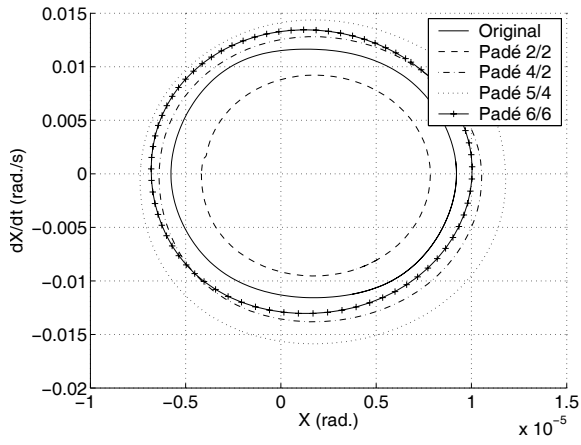


Figure 21: Limit cycle $(\theta_a, \dot{\theta}_a)$ for $\mu = 1.01\mu_0$

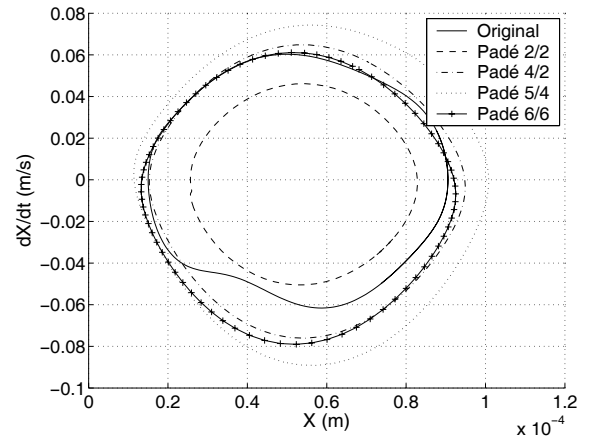


Figure 22: Limit cycle (z_a, \dot{z}_a) for $\mu = 1.01\mu_0$

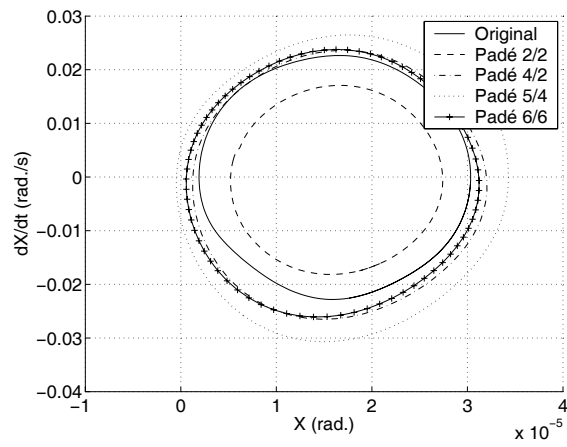


Figure 23: Limit cycle $(\psi_a, \dot{\psi}_a)$ for $\mu = 1.01\mu_0$

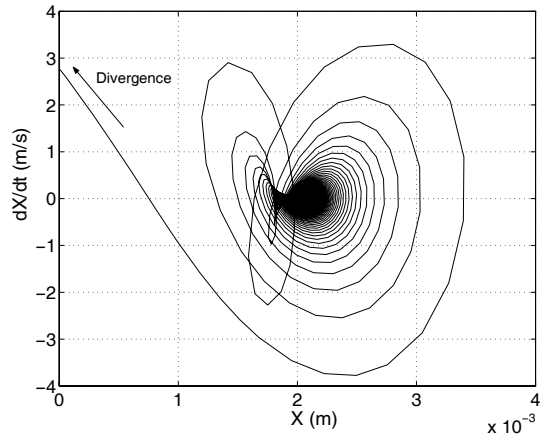


Figure 24: divergence for the limit cycle (x_s, \dot{x}_s)

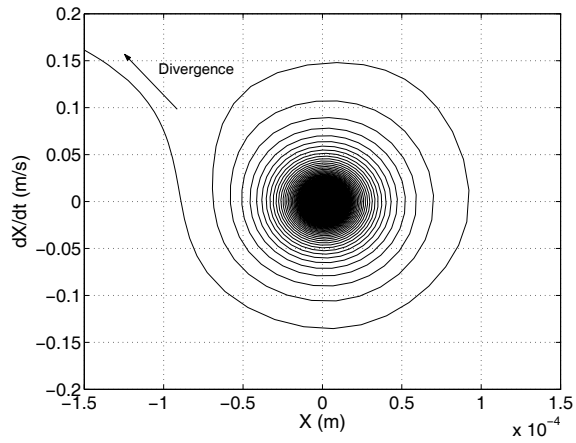


Figure 25: divergence for the limit cycle (y_b, \dot{y}_b)

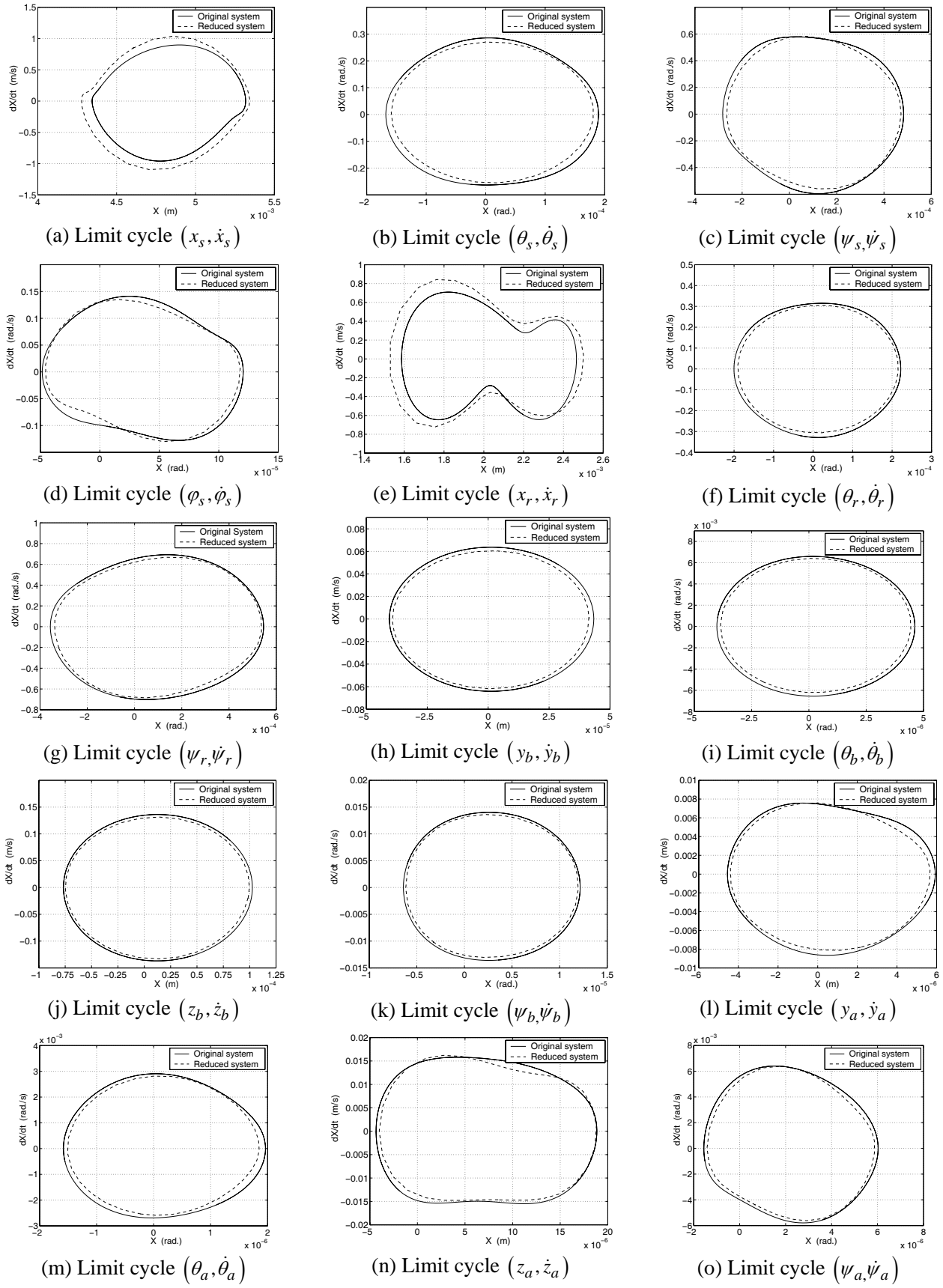


Figure 26: Comparison between the original and reduced system for $P/P_{\max}=0.1$